Original Article

Differential diagnosis of pulmonary nodular mucinous adenocarcinoma and tuberculoma with dynamic CT: a retrospective study

Yue-Hui Yin[1], Yuan-Gang Qi[2], Bing Wang[3]

[1]Department of Radiology, Weifang People's Hospital, Weifang, China; [2]Department of Radiology, Shandong Cancer Hospital and Institute, Shandong First Medical University and Shandong Academy of Medical Sciences, Jinan, China; [3]Department of Radiology, The Third Affiliated Hospital of Shandong First Medical University (Affiliated Hospital of Shandong Academy of Medical Sciences), Jinan, China

Contributions: (I) Conception and design: YH Yin, B Wang; (II) Administrative support: YH Yin, B Wang; (III) Provision of study materials or patients: YG Qi, YH Yin; (IV) Collection and assembly of data: B Wang; (V) Data analysis and interpretation: B Wang; (VI) Manuscript writing: All authors; (VII) Final approval of manuscript: All authors.

Correspondence to: Bing Wang. Department of Radiology, The Third Affiliated Hospital of Shandong First Medical University (Affiliated Hospital of Shandong Academy of Medical Sciences), 38# Wuyingshan Road, Jinan 250031, China. Email: bingshan2002@163.com.

Background: Pulmonary nodular mucinous adenocarcinoma (PNMA) tends to be easily misdiagnosed as tuberculoma in practice. In this study, we aimed to discriminate PNMA from tuberculoma with dynamic computed tomography (CT).

Methods: In this study, 38 consecutive pathologically confirmed cases of PNMA and 23 cases of tuberculoma from January 2015 to December 2019 were retrospectively collected. The mean CT attenuations of each lesion were examined. The values on the plain scan, the venous scan, and the enhanced values (CT attenuation of lesion of venous scan minus that of the plain scan) were tested with an independent *t*-test pair-wisely. Receiver operating characteristic (ROC) curve analyses were performed to test the differential diagnosis values. The presence of satellite lesions was determined with the chi-square test.

Results: The mean CT attenuation of tuberculoma shown on the plain scan was significantly higher than that of PNMA (35.15±16.00 *vs.* 24.00±12.67 HU; P<0.01). The enhanced value of tuberculoma on venous scan was significantly lower than that of PNMA (13.44±13.40 *vs.* 22.52±14.00 HU; P=0.02). The optimum CT attenuation of the plain scan and the enhanced value for differential diagnosis were 28.80 and 14.25 HU [area under the curve (AUC) =0.72, 95% confidence interval (CI): 0.58–0.86; and AUC =0.70, 95% CI: 0.59–0.84], with sensitivity (78.3% *vs.* 71.1%) and specificity (63.8% *vs.* 69.6%) respectively. The satellite lesions were more often observed in the tuberculoma group (P<0.01).

Conclusions: The CT attenuation of the plain scan, the enhanced value after enhancement, and the presence of satellite lesions might be useful in differentiating PNMA from tuberculoma.

Keywords: Computed tomography (CT); X-ray; pulmonary nodular mucinous adenocarcinoma (PNMA); tuberculoma

Submitted Jan 21, 2022. Accepted for publication Apr 15, 2022.
doi: 10.21037/jtd-22-372
View this article at: https://dx.doi.org/10.21037/jtd-22-372

Introduction

Lung cancer is a leading cause of death, leading to about 1.7 million deaths each year worldwide (1,2). Currently, research on diagnosis and treatment of lung cancer is a hot topic. Primary pulmonary mucinous adenocarcinoma (PPMA) has been classified as a special subtype of lung adenocarcinoma by World Health Organization in 2015 and by the American Lung Cancer Association/Thoracic

Society/European Respiratory Society in 2011. PPMA is rare in clinical practice and accounts for 0.25% of lung adenocarcinoma worldwide (3-6). Computed tomography (CT) is a mainstay for the diagnosis of PPMA. PPMA has diverse CT manifestations, including solid nodular, ground-glass nodular, inflammatory, and mixed types. Except for solid nodular type, other types of PPMA are relatively easily differentiated from lesions caused by inflammation and tuberculosis according to CT morphology and enhancement characteristics. However, the pulmonary nodular mucinous adenocarcinoma (PNMA), especially nodules with inconspicuous enhancement characteristics, smooth or speculated edges, internal vacuoles or cavities, or other characteristics, tend to be easily misdiagnosed. The PNMA may show no-mild enhancement, linear enhancement at the edges, or internal cord-like enhancement after enhancement on dynamic CT. In addition, PNMA may show no-mild uptake on positron-emission tomography (PET)/CT. The morphology and imaging features may overlap with a tuberculoma (7-9). In our department, many cases of PNMA were misdiagnosed as tuberculoma. Like other types of PPMA, PNMA also tend to be airborne, so early detection and differential diagnosis from tuberculoma are particularly important to avoid metastasis and achieve prompt treatment (7-9).

PPMA is rare in practice, therefore most existing literature were case reports and some reported as bronchoalveolar carcinoma, the former name of PPMA (10). As to PNMA, its imaging features have not been fully reported yet. In this study, we retrospectively analyzed the CT morphological and enhancement characteristics of PNMA and tuberculoma to improve understanding about how to tell the difference between them. We present the following article in accordance with the STARD reporting checklist (available at https://jtd.amegroups.com/article/view/10.21037/jtd-22-372/rc).

Methods

The study was conducted in accordance with the Declaration of Helsinki (as revised in 2013). The study was approved by the institutional review board of Weifang People's Hospital (No. WPHEC2022002003). Individual consent for this retrospective analysis was waived.

General information

Thirty-eight consecutive cases of PNMA and 23 cases of tuberculoma who were pathologically confirmed by surgery or needle biopsy from January 2015 to December 2019 in Weifang People's Hospital were retrospectively collected. The maximum diameter of the nodule was less than or equal to 3.0 cm; when its diameter was less than or equal to 1.0 cm, a 1.0 mm thin layer was built in the lung window and other stages. To be included in this study, PNMA met the following conditions: (I) no more than 10% of mucinous adenocarcinoma medium acinar or papillary adenocarcinoma components; (II) solitary and solid nodules, which may be associated with vacuoles and cavities, are not associated with bronchial inflation sign or ground-glass density; (III) no metastasis. To be included in the study, tuberculoma met the following conditions: (I) a solitary nodule; (II) the tuberculoma was not associated with exudative or proliferative lesions.

Among the PNMA patients, 19 were male and 19 were female. Of the tuberculoma patients, 17 were male and 6 were female. The oldest PNMA patient was 79 years old and the youngest was 42 years old; the oldest tuberculoma patient was 74 years old and the youngest was 39 years old.

Inspection method

Patients were examined with a 64- or 128-slice iCT scanner (Philips Medical, Eindhoven, Netherlands). Scanning parameters were setting as 120 kV, 200 mAs. The original acquisition slice thickness was 0.625 mm with a pitch of 1.5. Conventional scan slice thickness was 5 mm, and high-resolution CT (HRCT) reconstruction slice thickness and increment were both 1 mm. Proceeding with the algorithm "sharp YB". First, the patient was placed in the supine position with both hands holding their head. Patients were asked to hold their breath during the scan, with the scanning range from the apex of the lung to the dome of the diaphragm. Then, all patients were examined with a contrast-enhanced scan after the non-ionic contrast medium iohexol (Beijing Hokuriku Pharmaceutical Co., Ltd., China) (350 mg/mL) was injected into the antecubital vein at a dose of 80–100 mL and an injection rate of 3.0 mL/s. Scans were performed at arterial phase (30 s) and venous phase (90 s) after the injection of the contrast medium. Lung window was –600 HU with a window width of 1,600 HU. The mediastinal window was window 40 HU with a window width 400 HU.

Image analysis

Only venous phase CT values were measured and recorded

in this study because the lesions were fully enhanced at this stage. The mean CT value of the nodule on the plain scan and the venous scan were measured, and the enhanced values (CT attenuation of lesion of venous scan minus that of the plain scan) were calculated. To ensure the accuracy of data, the largest slice of the lesion and three adjacent slices above and below were selected as the region of interest (ROI) with the same size, avoiding any area with calcification, necrosis, and atelectasis. When the density was uniform, the area of the ROI was greater than half of the interface; when the density was uneven, it was necessary to select the slice with the most solid components to make a measurement and calculate its mean value according to the results of three measurements.

Two radiologists (more than 5 years of work experience) observed the presence or absence of satellite lesions around the nodules and counted them. Disagreement was resolved by negotiation. The satellite lesions were defined as: ≥1 miliary nodules around the nodules (within 3.0 cm), except for the only presence of miliary nodules distal to the nodules (possible obstructive inflammation).

Statistical analysis

SPSS 20.0 (IBM Corporation, Armonk, NY, USA) was used for the statistical tests. All numeric variables were first tested for normal distribution, and normal distribution data were expressed as mean ± standard deviation (SD). An independent sample *t*-test was used to compare the differences in lesion size, CT value on the plain and venous scan, and the enhanced values between the two groups. The incidence of perilesional satellite lesions was compared between the two groups using the chi-square test. Using receiver operating characteristic (ROC) curves, the optimal threshold for the differential diagnosis of each parameter and its sensitivity and specificity were determined. Area under the curve (AUC) >0.70 was considered to be acceptable. P<0.05 (two-sided) was considered statistically significant.

Results

Analysis results of basic characteristics of patients

The age and gender in the PNMA and tuberculoma groups were compared. The mean age was 58.68±9.36 in the PNMA group and 55.35±9.36 in the tuberculoma group (t=–1.33; P=0.19) after the *t*-test, which was not statistically significant. The male-to-female ratio was 19:19 in the PNMA group and 17:6 in the tuberculoma group. The chi-square test (χ^2=3.39; P=0.07) showed that gender was not significant between the two groups.

CT value comparison results of CT images

The mean CT value on the plain scan, the venous scan and the enhanced values between the two groups were compared, respectively. The mean CT attenuation on the plain scan of tuberculoma was significantly higher than that of PNMA (35.15±16.00 *vs.* 24.00±12.67 HU; P<0.01). The enhanced value of tuberculoma after enhancement was significantly lower than that of PNMA (13.44±13.40 *vs.* 22.52±14.00 HU; P=0.02). The mean CT value on the venous scan was comparable. PNMA had a lower density on the plain scan than tuberculoma, and tuberculoma had a lower enhanced value on the venous scan than PNMA (*Figures 1*,*2*, *Table 1*). ROC curves were generated by selecting each of the above statistically significant CT value parameters (*Table 2*).

Comparison results of satellite lesions in CT images

The proportions of CT lung window images with and without satellite lesions in patients of the PNMA group and the tuberculoma group were 3:35 and 13:10, respectively (χ^2=17.51; P<0.01), and the difference was statistically significant. The lung window images analysis showed that tuberculoma had more satellite lesions than PNMA.

Discussion

Although PNMA is rare and grows slowly, it's malignant and can invade lymph and blood vessels (11-13). However, PNMA can often be misdiagnosed on CT as tuberculoma, which is a benign lesion with high incidence. Current studies show that PNMA cannot be distinguished from tuberculoma based on clinical symptoms, gender, and age. For example, Masai *et al.* reported the male to female ratio of 2:1 (14). In this study, the male to female ratio of patients in the PNMA group was 1:1, and the male to female ratio of group was 17:6 in the tuberculoma group, indicating that gender is not a factor for distinguishing PNMA from tuberculoma. The age of patients in the PNMA group was 58.68±9.36, and the age of patients in the tuberculoma group was 55.35±9.36, which also indicated that age is not a distinguishing factor. Therefore, our data is consistent with

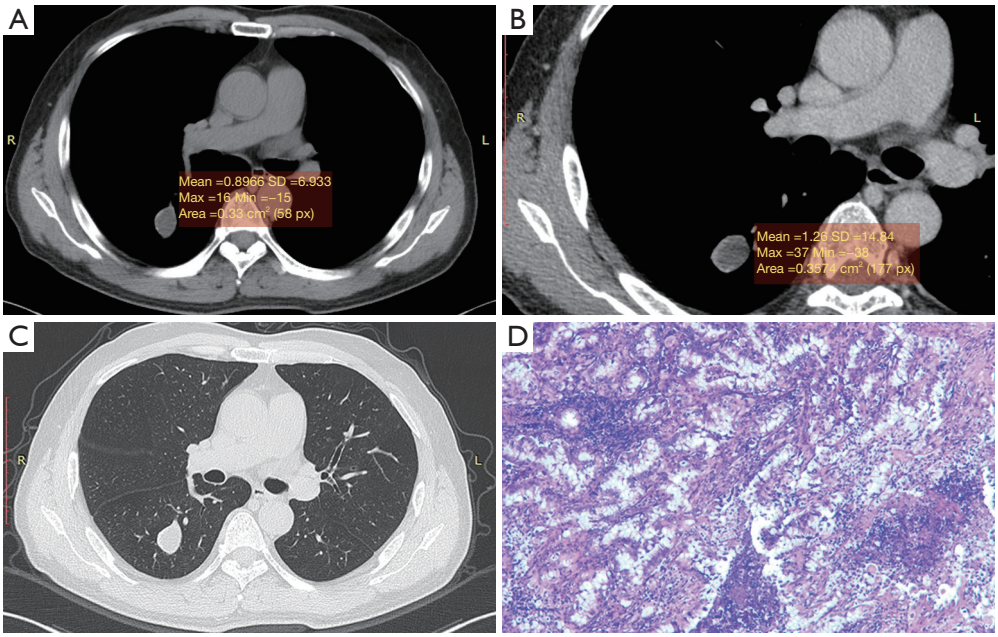

Figure 1 A 50-year-old male patient with PNMA of the right lower lobe was misdiagnosed as tuberculoma by CT. (A) the nodule was low-density on plain scan CT image; (B) the nodule showed thin linear enhancement at the edge and no enhancement in the center after enhancement; (C) CT lung window image showed no satellite lesion around the nodule; (D) pathologically confirmed PNMA (HE, ×10) without obvious intravascular tumor thrombus and cancer at the bronchial end. SD, standard deviation; PNMA, pulmonary nodular mucinous adenocarcinoma; CT, computed tomography; HE, hematoxylin and eosin.

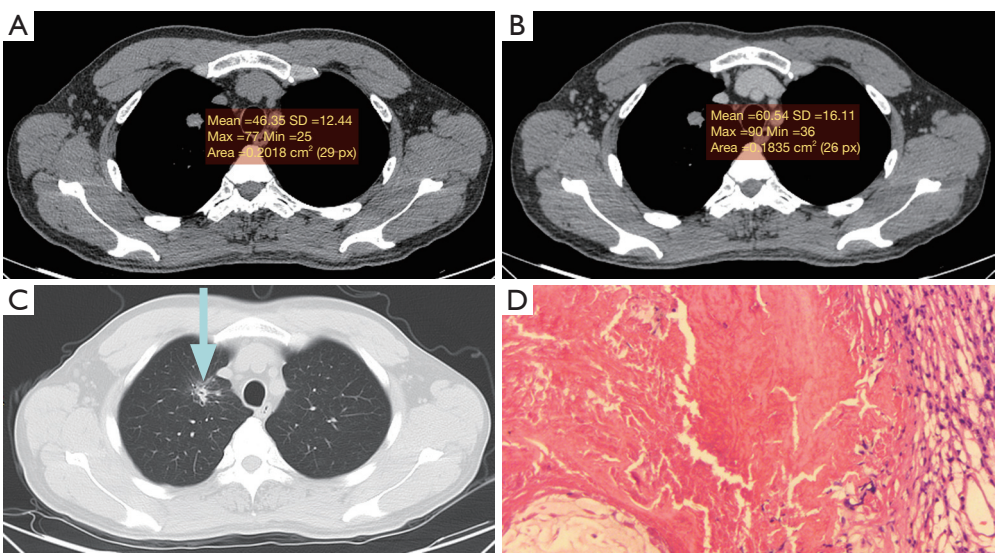

Figure 2 A 48-year-old male patient with tuberculoma in the right upper lobe, was misdiagnosed as PNMA by CT. (A) CT image of plain scan, CT value was 46.35 HU; (B) CT image in venous phase, CT value was 60.54 HU; (C) CT lung window image, satellite lesions were seen around the nodules (the arrow); (D) pathological image (HE, ×10), chronic granulomatous inflammation with caseous necrosis, with a high possibility of tuberculoma. SD, standard deviation; PNMA, pulmonary nodular mucinous adenocarcinoma; CT, computed tomography; HE, hematoxylin and eosin.

Table 1 Comparison of the mean CT value in the plain and venous scan, and the enhanced value of PNMA and tuberculoma

CT density (HU)	PNMA group (n=38)	Tuberculoma group (n=23)	*t*	P
Plain scan	24.00±12.67	35.15±16.00	3.02	<0.01
Venous scan	47.67±25.08	49.61±20.53	0.31	0.76
Enhanced value	22.52±13.99	13.44±13.39	−2.49	0.02

CT, computed tomography; PNMA, pulmonary nodular mucinous adenocarcinoma.

Table 2 ROC analysis of the CT value of plain scan and the enhanced value after enhancement between PNMA and tuberculoma

Diagnostic index	AUC	Threshold	Sensitivity (%)	Specificity (%)
CT value of plain scan	0.721	28.80	78.3	63.8
CT enhanced value	0.697	14.25	71.1	69.6

ROC, receiver operating characteristic; CT, computed tomography; PNMA, pulmonary nodular mucinous adenocarcinoma; AUC, area under the curve.

the previous findings in other reports.

Histologically, PNMA was reported to be composed of densely packed mucin-rich tumor cells, with central fibrosis and alveolar spaces filled with mucin (15,16). Tuberculoma is formed by fibrous tissue containing caseous necrotic tissue. Because both of them are low-density on plain scan, and their morphological characteristics overlap greatly, one is easily misdiagnosed as the other. In this study, tuberculoma was misdiagnosed as PNMA in 17 of 23 cases with a misdiagnosis rate of 73.9%, and PNMA was misdiagnosed as tuberculoma or inflammation in 10 of 38 cases with a misdiagnosis rate of 26.3%.

CT is a commonly used method for the diagnosis of lung cancer and tuberculosis. Some reports (17,18) found that the CT value of lung cancer at the level of 40–70 Kev was higher than that of the tuberculosis group in the quantitative analysis of peripheral lung cancer and tuberculoma by energy spectrum. There were many reports on PET/CT for PPMA (19,20), but there were no reports about CT features of PNMA and tuberculoma. In this study, we found that the CT value of tuberculoma on plain scan was 35.15±16.00, and the CT value of PNMA was 24.00±12.67. The CT value of the tuberculoma group on plain scan was generally higher than that of the PNMA group, which is inconsistent with a former report (17). This may be caused by the different pathological types and research methods of PNMA. Tuberculoma is formed by fibrous tissue containing caseous necrotic tissue with low density, but calcification can easily occur. Some calcifications are fine sand and scattered, which easily leads to a higher value of CT measurement. PNMA is a mixture of mucin-rich tumor cells, fibrous tissue, and alveolar spaces filled with mucin-protein, generally with fewer fibrous components, which may lead to low CT value (14,15). By ROC curve comparison, we found that the threshold of CT value on plain scan in the differential diagnosis of tuberculoma and PNMA is 28.8 HU, the sensitivity is 78.3%, and the specificity is 63.8%. The specificity of diagnosis was not very high, so some false positives may exist when setting a CT value of 28.8 HU to distinguish between tuberculoma and PNMA. This relatively low specificity may occur because of the limited number of collected samples. Therefore, more samples need to be included future research.

CT dynamic contrast-enhanced scan is also an important method to diagnose PNMA and tuberculoma. Swensen *et al.* found that tuberculoma had no significant enhancement and the CT enhanced value was <20 HU (21). However, Yi *et al.* found that some tuberculomas had significant enhancement, which was similar to the enhancement pattern of some lung cancer (22). Currently, agreement has not been reached on the mode of tuberculoma enhancement. In this study, we collected 23 cases of tuberculoma including 7 cases with obvious enhancement (CT enhanced value >20 HU) and 16 cases with no-mild enhancement. Our findings were consistent with those reported by Chae *et al.* (23), who showed that the CT enhanced value after enhancement was higher in the lung cancer group than that in the tuberculosis group, but the difference between PNMA and tuberculoma was not reported.

Only venous phase CT values were measured and recorded in this study because the lesions were fully enhanced at this stage. The CT value of the venous phase was 47.67±25.08 HU in the PNMA group and 49.61±20.53 HU in the tuberculoma group. It is not significant in the CT value of the venous phase between the two groups. The enhanced value of venous phase was 22.52±13.99 HU in the PNMA group and 13.44±13.39 HU in the tuberculoma group. The enhanced value in the PNMA group was higher than that in the tuberculoma group. The pathological characteristics of the lesion determined the enhancement patterns. The center of tuberculoma is caseous necrotic tissue without blood

supply, the periphery is a capsule, and the inner layer of the capsule is granulation tissue containing blood supply. Therefore, according to the degree of caseous necrosis and the amount of granulation tissue, the enhancement mode is non-enhanced, annular, strip, linear or other forms (24). PNMA is composed of a mixture of mucin-rich tumor cells, fibrous tissue, and alveolar spaces filled with mucin. According to the amount of solid component, fibrous tissue and mucinous components, the tumor showed a complex enhancement pattern. Moreover, papillary or alveolar components within PNMA increased the difference of CT features. In this study, we also found that the threshold of CT enhanced value in the differential diagnosis between tuberculoma and PNMA is 14.25 HU, with a sensitivity of 71.1% and a specificity of 69.6% by comparison of ROC curves. The specificity and sensitivity were not very high, which may be led by the small difference in venous phase CT values between the two groups, and further study with an increasing sample size is needed.

Tuberculoma is often accompanied with satellite lesions. In this study, 13 of 23 tuberculomas had satellite lesions, with a ratio of 13:10. In comparison, 3 of 38 PNMA had satellite lesions, with a ratio of 3:35. Thus, there was statistical significance between the two groups. These data indicate that tuberculomas have more common satellite lesions than PNMA, which is consistent with previous reports (25,26).

Our study has some limitations: (I) PNMA is rare in practice. We searched our database thoroughly and only 38 cases of PNMA matched our criteria, so our sample was small; (II) the density of the selected nodule part was uneven, and the measurement of CT value may cause certain errors; and (III) it is a retrospective study, so there was some bias in selecting cases. Future research should increase the sample size and strictly select the case criteria for further study.

Conclusions

In conclusion, the CT value of plain scan, the enhanced value after enhancement, and satellite lesions around nodules might be useful in differentiating PNMA from tuberculoma.

Acknowledgments

Funding: None.

Footnote

Reporting Checklist: The authors have completed the STARD reporting checklist. Available at https://jtd.amegroups.com/article/view/10.21037/jtd-22-372/rc

Data Sharing Statement: Available at https://jtd.amegroups.com/article/view/10.21037/jtd-22-372/dss

Conflicts of Interest: All authors have completed the ICMJE uniform disclosure form (available at https://jtd.amegroups.com/article/view/10.21037/jtd-22-372/coif). The authors have no conflicts of interest to declare.

Ethical Statement: The authors are accountable for all aspects of the work in ensuring that questions related to the accuracy or integrity of any part of the work are appropriately investigated and resolved. The study was conducted in accordance with the Declaration of Helsinki (as revised in 2013). The study was approved by the institutional review board of Weifang People's Hospital (No. WPHEC2022002003). Individual consent for this retrospective analysis was waived.

References

1. Siegel RL, Miller KD, Jemal A. Cancer statistics, 2019. CA Cancer J Clin 2019;69:7-34.
2. Bray F, Ferlay J, Soerjomataram I, et al. Global cancer statistics 2018: GLOBOCAN estimates of incidence and mortality worldwide for 36 cancers in 185 countries. CA Cancer J Clin 2018;68:394-424.
3. Travis WD, Brambilla E, Noguchi M, et al. International association for the study of lung cancer/american thoracic society/european respiratory society international multidisciplinary classification of lung adenocarcinoma. J Thorac Oncol 2011;6:244-85.

4. Travis WD, Brambilla E, Burke AP, et al. Introduction to The 2015 World Health Organization Classification of Tumors of the Lung, Pleura, Thymus, and Heart. J Thorac Oncol 2015;10:1240-2.
5. Travis WD, Brambilla E, Burke AP, et al. WHO classification of tumours of the lung, pleura, thymus and heart. 4th ed. Lyon: IARC Publications, 2015.
6. Türüt H, Demirag F, Gulhan E, et al. Primary pulmonary mucinous adenocarcinoma in a 15-year-old boy. Eur J Cardiothorac Surg 2006;29:851-3.
7. Gaeta M, Blandino A, Pergolizzi S, et al. Patterns of recurrence of bronchioloalveolar cell carcinoma after surgical resection: a radiological, histological, and immunohistochemical study. Lung Cancer 2003;42:319-26.
8. Oka S, Hanagiri T, Uramoto H, et al. Surgical resection for patients with mucinous bronchioloalveolar carcinoma. Asian J Surg 2010;33:89-93.
9. Gemma A, Noguchi M, Hirohashi S, et al. Clinicopathologic and immunohistochemical characteristics of goblet cell type adenocarcinoma of the lung. Acta Pathol Jpn 1991;41:737-43.
10. Lee HY, Cha MJ, Lee KS, et al. Prognosis in Resected Invasive Mucinous Adenocarcinomas of the Lung: Related Factors and Comparison with Resected Nonmucinous Adenocarcinomas. J Thorac Oncol 2016;11:1064-73.
11. Lee HY, Lee KS, Han J, et al. Mucinous versus nonmucinous solitary pulmonary nodular bronchioloalveolar carcinoma: CT and FDG PET findings and pathologic comparisons. Lung Cancer 2009;65:170-5.
12. Edge SB, Compton CC. The American Joint Committee on Cancer: the 7th edition of the AJCC cancer staging manual and the future of TNM. Ann Surg Oncol 2010;17:1471-4.
13. Erasmus JJ, Connolly JE, McAdams HP, et al. Solitary pulmonary nodules: Part I. Morphologic evaluation for differentiation of benign and malignant lesions. Radiographics 2000;20:43-58.
14. Masai K, Sakurai H, Suzuki S, et al. Clinicopathological features of colloid adenocarcinoma of the lung: A report of six cases. J Surg Oncol 2016;114:211-5.
15. Yap CS, Schiepers C, Fishbein MC, et al. FDG-PET imaging in lung cancer: how sensitive is it for bronchioloalveolar carcinoma? Eur J Nucl Med Mol Imaging 2002;29:1166-73.
16. Sawada E, Nambu A, Motosugi U, et al. Localized mucinous bronchioloalveolar carcinoma of the lung: thin-section computed tomography and fluorodeoxyglucose positron emission tomography findings. Jpn J Radiol 2010;28:251-8.
17. Lin JZ, Zhang L, Zhang CY, et al. Application of Gemstone Spectral Computed Tomography Imaging in the Characterization of Solitary Pulmonary Nodules: Preliminary Result. J Comput Assist Tomogr 2016;40:907-11.
18. Wang SY, Gao JB, Zhang R, et al. Value of gemstone spectral CT imaging in diagnosis of solitary pulmonary nodule. Zhonghua Yi Xue Za Zhi 2016;96:1040-3.
19. Chang JM, Lee HJ, Goo JM, et al. False positive and false negative FDG-PET scans in various thoracic diseases. Korean J Radiol 2006;7:57-69.
20. Cha MJ, Lee KS, Kim TJ, et al. Solitary Nodular Invasive Mucinous Adenocarcinoma of the Lung: Imaging Diagnosis Using the Morphologic-Metabolic Dissociation Sign. Korean J Radiol 2019;20:513-21.
21. Swensen SJ, Brown LR, Colby TV, et al. Lung nodule enhancement at CT: prospective findings. Radiology 1996;201:447-55.
22. Yi CA, Lee KS, Kim EA, et al. Solitary pulmonary nodules: dynamic enhanced multi-detector row CT study and comparison with vascular endothelial growth factor and microvessel density. Radiology 2004;233:191-9.
23. Chae EJ, Song JW, Seo JB, et al. Clinical utility of dual-energy CT in the evaluation of solitary pulmonary nodules: initial experience. Radiology 2008;249:671-81.
24. Jeong YJ, Lee KS. Pulmonary tuberculosis: up-to-date imaging and management. AJR Am J Roentgenol 2008;191:834-44.
25. Zhuo Y, Zhan Y, Zhang Z, et al. Clinical and CT Radiomics Nomogram for Preoperative Differentiation of Pulmonary Adenocarcinoma From Tuberculoma in Solitary Solid Nodule. Front Oncol 2021;11:701598.
26. Zhang J, Han T, Ren J, et al. Discriminating Small-Sized (2 cm or Less), Noncalcified, Solitary Pulmonary Tuberculoma and Solid Lung Adenocarcinoma in Tuberculosis-Endemic Areas. Diagnostics (Basel) 2021;11:930.

(English Language Editor: C. Mullens)

Cite this article as: Yin YH, Qi YG, Wang B. Differential diagnosis of pulmonary nodular mucinous adenocarcinoma and tuberculoma with dynamic CT: a retrospective study. J Thorac Dis 2022;14(4):1225-1231. doi: 10.21037/jtd-22-372